JOURNAL OF GEOPHYSICAL RESEARCH, VOL. 112, D10S31, doi:10.1029/2006JD007588, 2007

Cloud condensation nuclei closure during the International Consortium for Atmospheric Research on Transport and Transformation 2004 campaign: Effects of size-resolved composition

Jeessy Medina,[1] Athanasios Nenes,[2] Rafaella-Eleni P. Sotiropoulou,[3] Laura D. Cottrell,[4] Luke D. Ziemba,[4] Pieter J. Beckman,[4] and Robert J. Griffin[5]

Received 31 May 2006; revised 10 November 2006; accepted 4 December 2006; published 23 February 2007.

[1] Measurements of cloud condensation nuclei (CCN), aerosol size distribution and chemical composition were obtained at the UNH-AIRMAP Thompson Farms site, during the ICARTT 2004 campaign. This work focuses on the analysis of a week of measurements, during which semiurban and continental air were sampled. Predictions of CCN concentrations were carried out using ''simple'' Köhler theory; the predictions are subsequently compared with CCN measurements at 0.2%, 0.3%, 0.37%, 0.5% and 0.6% supersaturation. Using size-averaged chemical composition, CCN are substantially overpredicted (by 35.8 ± 28.5%). Introducing size-dependent chemical composition substantially improved closure (average error 17.4 ± 27.0%). CCN closure is worse during periods of changing wind direction, suggesting that the introduction of aerosol mixing state into CCN predictions may sometimes be required. Finally, knowledge of the soluble salt fraction is sufficient for description of CCN activity.

Citation: Medina, J., A. Nenes, R.-E. P. Sotiropoulou, L. D. Cottrell, L. D. Ziemba, P. J. Beckman, and R. J. Griffin (2007), Cloud condensation nuclei closure during the International Consortium for Atmospheric Research on Transport and Transformation 2004 campaign: Effects of size-resolved composition, *J. Geophys. Res.*, *112*, D10S31, doi:10.1029/2006JD007588.

1. Introduction

[2] It is well accepted that aerosol-cloud-climate interactions constitute a major source of uncertainty for assessments of anthropogenic climate change [*Intergovernmental Panel on Climate Change (IPCC)*, 2001; *Charlson et al.*, 1992; *Haywood and Boucher*, 2000; *Ramanathan et al.*, 2001]. Understanding what controls the ability of ambient atmospheric aerosol to act as cloud condensation nuclei (CCN) is at the heart of this problem, as all physically based treatments of cloud droplet formation in global climate models [e.g., *Abdul-Razzak and Ghan*, 2000, 2002; *Nenes and Seinfeld*, 2003; *Fountoukis and Nenes*, 2005] rely on predictions of CCN concentrations.

[3] It is necessary to expose the particle to a supersaturation long enough for it to reach its critical radius. Each aerosol, when exposed to a water vapor supersaturation above a characteristic ''critical'' supersaturation, s_c, experiences unconstrained growth or, acts as a CCN and forms a cloud droplet. s_c depends on the aerosol dry size and chemical composition, and is computed from thermodynamic arguments first introduced by H. Köhler [*Köhler*, 1921, 1936]. This ''Köhler theory,'' originally developed to describe the CCN activity of salt particles, has since been refined to address the behavior of multicomponent atmospheric aerosol. As a result, theory can be quite complex and may require the knowledge of poorly constrained parameters. This is especially true if the aerosol contains substantial amounts of water-soluble organic carbon (WSOC). WSOC can act as a surfactant [*Decesari et al.*, 2003], potentially depressing droplet surface tension [*Facchini et al.*, 1999] and the condensation rate of water [e.g., *Nenes et al.*, 2002]. WSOC may also contribute solute [*Shulman et al.*, 1996], although low solubility [e.g., *Nenes et al.*, 2002], dissolution kinetics (A. Asa-Awuku and A. Nenes, CCN predictions: Is theory sufficient for assessments of the indirect effect?, submitted to *Journal of Geophysical Research*, 2006) and the presence of soluble salts can diminish its importance. Since each of these effects alone can either enhance or diminish the CCN activity of the aerosol, comprehensively treating the effect of organics on CCN activation can be quite complex and subject to substantial uncertainty.

[4] ''CCN closure,'' or comparison of predictions with observations of CCN concentrations, is the ultimate test of

[1]School of Chemical and Biomolecular Engineering, Georgia Institute of Technology, Atlanta, Georgia, USA.
[2]Schools of Earth and Atmospheric Sciences and Chemical and Biomolecular Engineering, Georgia Institute of Technology, Atlanta, Georgia, USA.
[3]School of Earth and Atmospheric Sciences, Georgia Institute of Technology, Atlanta, Georgia, USA.
[4]Institute for the Study of Earth, Oceans, and Space, University of New Hampshire, Durham, New Hampshire, USA.
[5]Institute for the Study of Earth, Oceans, and Space, and Department of Earth Sciences, University of New Hampshire, Durham, New Hampshire, USA.

0148-0227/07/2006JD007588$09.00

Köhler theory and has been the focus of numerous studies. *Liu et al.* [1996] made ground measurements of CCN at Chebogue Point in 1993 as part of the North Atlantic Regional Experiment (NARE) intensive. CCN at 0.4% were measured using a static-diffusion cloud chamber from DH Associates. CCN were predicted using size distributions from a PMS passive cavity aerosol spectrometer probe (PCASP-100X). Aerosol composition was obtained from filter samples. Two distinct groups of aerosols were identified, one likely from cloud processing; despite this heterogeneity, good closure (i.e., within experimental uncertainty) was achieved for 75% of the time.

[5] *Covert et al.* [1998] conducted ground-based CCN measurements at 0.5% supersaturation using a thermal-gradient diffusion cloud chamber during the First Aerosol Characterization Experiment (Cape Grim, Tasmania, 1995). Differential mobility particle sizers were used to measure the size distribution. On average, *Covert et al.* [1998] obtained good closure, with a slight (20%) tendency for overprediction.

[6] During the second Aerosol Characterization Experiment (ACE-2) over the northeast Atlantic (Tenerife, Spain), *Chuang et al.* [2000a] made airborne CCN measurements onboard the CIRPAS Pelican. During this study, the Caltech continuous-flow CCN counter [*Chuang et al.*, 2000b] measured CCN at 0.1% supersaturation; size distributions were obtained with the Caltech Automated Classified Aerosol Detector (ACAD) [*Collins et al.*, 2000] along side a Particle Measuring Systems PCASP-100X. Chemical composition was not measured in situ but constrained from ground-based filter samples. Closure was not achieved, as the CCN concentration was overpredicted by more than tenfold.

[7] Ground-based CCN measurements were performed by *Cantrell et al.* [2001] at the Kaashidhoo Climate Observatory during the Indian Ocean Experiment (INDOEX) intensive field phase (February–March 1999). Aerosol chemical composition was obtained using an aerosol time-of-flight spectrometer (ATOFMS) and four micro-orifice uniform deposit cascade impactors (MOUDIs); aerosol size distributions were measured using a TSI SMPS. CCN spectra were obtained using a CCN Remover [*Ji et al.*, 1998], operated in series with the SMPS. Closure was achieved in 8 out the 10 cases; discrepancies increased with organic mass fraction.

[8] *Roberts et al.* [2003] performed measurements during the Cooperative LBA (Large-scale Biosphere-Atmosphere Experiment in Amazonia) Airborne Regional Experiment 1998 (CLAIRE-98). Ground measurements of CCN spectra were made using a thermal diffusion cloud chamber for supersaturations between 0.15 and 1.5%. Additional instrumentation included a multistage cascade impactor to determine chemical composition and a scanning mobility particle sizer to determine aerosol size distributions. The CCN activity of the LBA aerosol depended primarily on the aerosol soluble fraction; potential impact of surface tension depression from the presence of WSOC (assessed by applying the correlation of *Facchini et al.* [1999]), was found to be important only at low supersaturations.

[9] *Snider et al.* [2003] and *Dusek et al.* [2003] analyzed aerosol samples for CCN closure during the ACE-2 campaign. *Snider et al.* [2003] compared observations for 5 study days collected at a coastal site and on an aircraft over the eastern Atlantic Ocean. After accounting for differences between the mobility and sphere-equivalent diameters, CCN agreed with predictions for two sampling days unaffected by continental pollution. *Dusek et al.* [2003] analyzed data collected in southern Portugal and showed that WSOC constituents at the location constituted less than 10% of the total aerosol mass and neglected their effect on CCN activity. Despite this, calculated CCN were overestimated on average by 30%, comparable to the measurement and prediction uncertainty.

[10] *VanReken et al.* [2003] performed airborne CCN measurements during the Cirrus Regional Study of Tropical Anvils and Cirrus Layers–Florida Area Cirrus Experiment (CRYSTAL-FACE) field campaign (July 2002). Using two continuous-flow streamwise temperature gradient chambers [*Roberts and Nenes*, 2005], CCN were measured at 0.2 and 0.85% supersaturation. The aerosol was most frequently marine; assuming a composition of ammonium sulfate, closure was achieved to within 5% at 0.2% supersaturation, and 9% at 0.85% supersaturation.

[11] *Rissman et al.* [2006] performed an inverse aerosol-CCN closure and explored its sensitivity to chemical composition and mixing state. The observations were obtained during the 2003 atmospheric radiation measurement (ARM) aerosol intensive observational period (IOP) at the southern great plains (SGP) site in Oklahoma. Optimum closure was achieved when the population of aerosol is treated as an external mixture of particles, with the insoluble material preferentially distributed in particles less than 50 nm diameter.

[12] *Broekhuizen et al.* [2006] measured CCN concentrations using a continuous thermal-gradient diffusion chamber in Toronto, Canada. The CCN chamber measured CCN concentrations at 0.58% for 4 days. Aerosol size distributions were measured using a TSI SMPS and an APS system; chemical composition was simultaneously measured with an Aerodyne aerosol mass spectrometer (AMS). Considering the size-dependent composition, and assuming internally mixed aerosol, closure (on average) was achieved to within 4%.

[13] *Stroud et al.* [2006] measured aerosol size distribution with a TSI SMPS, chemical composition with an AMS and CCN concentration with a University of Wyoming thermal-gradient static-diffusion cloud chamber (CCNC-100A) [*Delene and Deshler*, 2000] during the Chemical Emission, Loss, Transformation and Interactions with Canopies (CELTIC) field program at Duke Forest in North Carolina. A numerical model of the CCN instrument [*Nenes et al.*, 2001] was used to perform an aerosol-CCN closure study, and to constrain the value of the water vapor mass uptake coefficient. CCN predictions were within a factor of two of the observations. Sensitivity simulations suggest that assuming either an insoluble organic fraction or external aerosol mixing were both sufficient assumptions to reconcile the model bias. The chamber model best reproduced the kinetics of droplet growth (i.e., timescale required for the scattering signal in the instrument view volume to peak) when the water vapor mass uptake coefficient was set equal to 0.07; this conclusion was insensitive to the assumption of chemical composition (or the degree of closure).

[14] Despite the numerous CCN studies, a comprehensive CCN climatology is still lacking. There is a strong need for CCN closure studies that cover a wide range of seasons and aerosol types; this precludes a robust quantification of CCN prediction uncertainty, especially for simplifying assumptions (e.g., aerosol mixing state, variation of composition with size and affinity of carbonaceous material with water) commonly taken in global models. This study, together with the work of *Broekhuizen et al.* [2006] and *Stroud et al.* [2006] is a step toward addressing this problem. We perform a detailed CCN closure study using concurrent measurements of aerosol size distribution, chemical composition and CCN concentrations during the New England Air Quality Study–Intercontinental Transport and Chemical Transformation 2004 (NEAQS-ITCT 2004) as part of the International Consortium for Atmospheric Research on Transport and Transformation (ICARTT). ICARTT was a series of coordinated experiments, focused on understanding the properties of regional aerosol and their effects on regional air quality and climate. NEAQS-ITCT 2004 took place during the months of July and August and focused on air quality along the Eastern Seaboard and the aging of North American emissions as they are transported out into the North Atlantic. This paper focuses on the importance of having size-resolved chemical composition on CCN closure; a companion paper (A. Nenes and J. Medina, manuscript in preparation, 2006) presents measurements of size-resolved CCN activity which are then used to gain insight on the characteristics of the aerosol organic species, infer the CCN mixing state and explore compositional effects on droplet growth kinetics. The main difference between this study and previous work [e.g., *Broekhuizen et al.*, 2006; *Stroud et al.*, 2006], is that it refers to a different location (in space and time) with aerosol exposed to a different mix of influences.

2. Observational Data Set

2.1. Study Location

[15] The measurements were obtained at the University of New Hampshire (UNH) Thompson Farm (TF) AIRMAP Observing Station (http://airmap.unh.edu/). The site is located in Durham, NH, approximately two miles south of the University of New Hampshire (43.11N, 70.95W, elevation 75 ft). TF is characterized by fields and surrounding forest with some local anthropogenic influence. The aerosol at this location is a complex mixture of organic and inorganic material and is ideal for a CCN closure study. Measurements for this campaign were done from late July to mid-August. This study focuses on a week of measurements, from 5 to 11 August 2004.

2.2. Instrumentation Setup

[16] Figure 1 is a schematic of the field instrumentation setup. A Droplet Measurement Technologies (DMT) streamwise thermal-gradient cloud condensation nuclei counter [*Roberts and Nenes*, 2005; *Lance et al.*, 2006] was used to measure CCN concentrations. A scanning mobility particle sizer (SMPS, TSI 3080) composed of a condensation particle counter (CPC, TSI 3010) and a long differential mobility analyzer (DMA, TSI 3081L) measured the dry aerosol size distribution. An Aerodyne Aerosol Mass Spectrometer (AMS) concurrently measured aerosol chemical composition. Air was drawn from the top of a 60 ft tower with a 2.5 μm URG cyclone at 10 L min^{-1} through a $\frac{1}{2}''$ OD copper tube. Inlet air sampled from atop a 60 ft tower was split into two flows, one for measurements of size-resolved chemical composition (AMS) and the other for measurements of size distribution (SMPS) and CCN activity (CFSTGC).

2.3. AMS Chemical Composition Measurements

[17] The AMS [*Jayne et al.*, 2000] can measure the aerosol size distribution (aerodynamic diameter) and chemical composition. Aerosol entering the instrument passes through a critical orifice and is aerodynamically focused into a narrow particle beam. The particles subsequently pass through a rotating chopper and are sized according to their time-of-flight across a vacuum chamber. After sizing, the particle beam is directed on resistively heated surface; particles are then vaporized and ionized with a 70 eV electron impact ionization source. The ions are filtered and detected with a quadrupole mass spectrometer and secondary electron multiplier. During ICARTT, the AMS was operated with a 130 μm diameter critical orifice and a 1% chopper rotating at approximately 100 Hz. The vaporizer was maintained at 550°C. The chemical composition and size distribution of the aerosol was alternately measured every 30 s and averaged data was saved every 10 min.

[18] Mass loadings for sulfate, nitrate, ammonium and organics were calculated according to *Allan et al.* [2003]. On the basis of findings from other aerosol instruments with similar size cuts [e.g., *Alfarra et al.*, 2004; *Zhang et al.*, 2005], a 50% collection efficiency is assumed (the rest of the particles being lost to particle bouncing). The collection efficiency used is consistent with concurrent 24 hour bulk filter measurements (L. Cottrell et al., manuscript in preparation, 2006). The collection efficiency is likely the largest source of uncertainty for AMS measurements [*Alfarra et al.*, 2004; *Zhang et al.*, 2005], as it has been found to vary with factors such as composition, relative humidity, and aerosol acidity. The relative ionization efficiency of different compounds has been characterized in other studies [*Jimenez et al.*, 2003; *Alfarra et al.*, 2004] and is thought to be related to the electron impact cross section of each compound. In this study, relative ionization efficiencies of 1.4, 1.2, and 4.0 were adapted for organics, sulfate, and ammonium, respectively. Size calibrations were performed using NIST traceable polystyrene latex spheres at the start of the campaign. Mass calibrations were performed using classified ammonium nitrate aerosol every 3 to 5 days throughout the campaign. AMS configuration, operation, and data are detailed by L. Cottrell et al. (manuscript in preparation, 2006).

2.4. Dry Size Distribution Measurements

[19] The TSI 3080 SMPS is an electrical mobility based system capable of high-resolution size distribution measurements. Figure 1 illustrates its major components. Dried ambient aerosol is charged using a Kr-85 neutralizer (TSI 3077A). The charged aerosol stream enters a DMA where aerosols are classified based upon their electrical mobility and counted with a TSI 3010 condensation particle counter (CPC). The DMA voltage can be scanned and a particle size

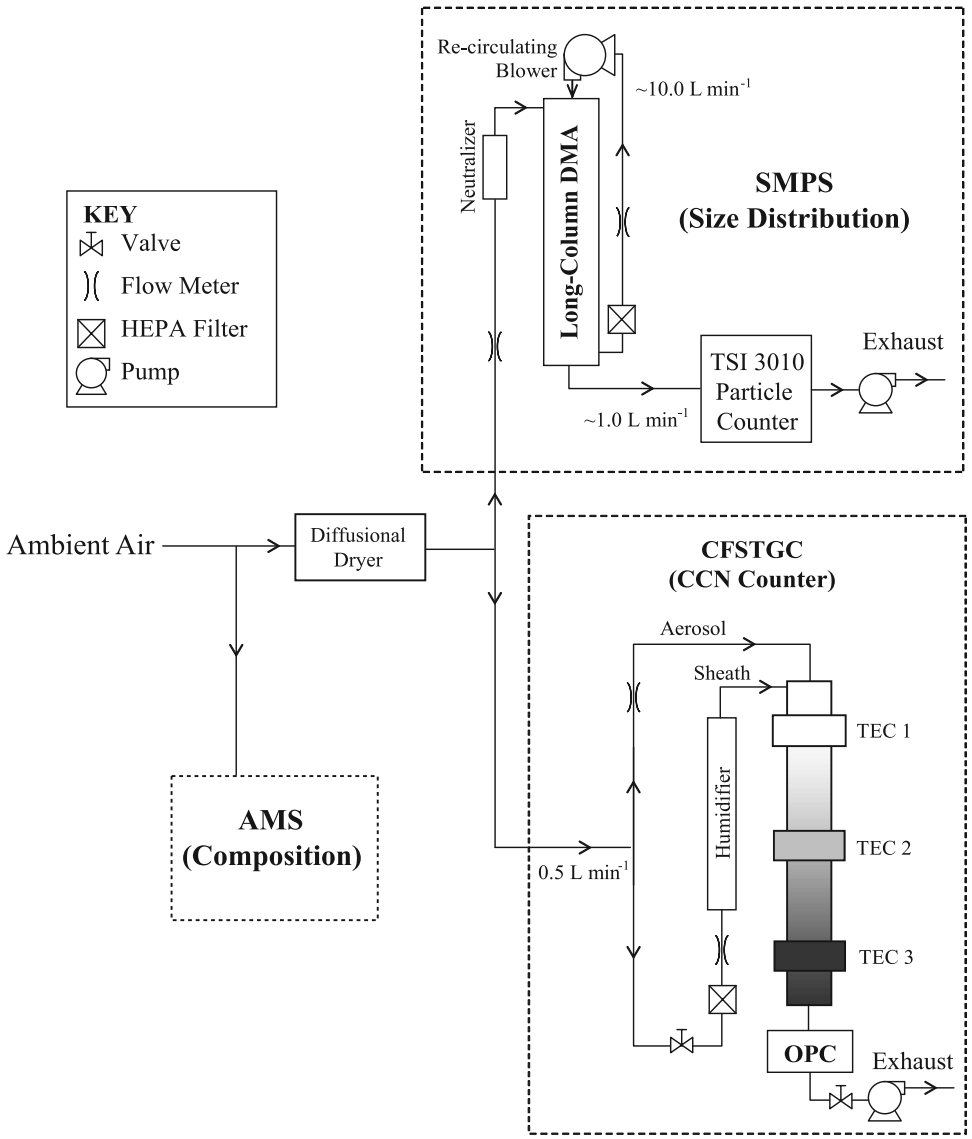

Figure 1. Schematic of the setup used for measuring the aerosol size distribution (SMPS), chemical composition (AMS) and CCN concentration (CFSTGC).

distribution is obtained for mobility diameters between 10 and 300 nm. Throughout this study, size distribution scans were obtained every 135 s (120 s for the voltage "upscan" and 15 s for the voltage "downscan"). The sample flow rate was set to 1 L min^{-1} and the sheath-to-aerosol flow was maintained at 10:1.

2.5. CCN Measurements

[20] The DMT CCN counter [*Roberts and Nenes*, 2005; *Lance et al.*, 2006] is a cylindrical continuous-flow streamwise thermal-gradient diffusion chamber. A constant streamwise temperature gradient is applied at the instrument walls; a constant centerline supersaturation develops from the difference between thermal and water vapor diffusivity. The instrument is able to generate supersaturations between 0.07% and 3% through precise control of the air flow and the streamwise temperature gradient. Figure 1 illustrates the components and flow diagram of the CCN instrument. The inlet flow is first split into a "sheath" and a "sample" flow. The "sample" is directed to the center of the flow column, whereas the "sheath" flow is filtered and humidified prior to its entry in the chamber, resulting in a "blanket" of humidified clean air around the "sample" flow. Both flows travel through the column exposing aerosol to a constant supersaturation. Aerosol whose s_c is below the instrument supersaturation will activate into droplets. An Optical Particle Counter (OPC) counts and sizes the droplets at the outlet of the column, using a 50 mW, 658 nm laser diode. All scattered light between 35° to 145° is collected and detected with a photodiode. A multichannel analyzer bins the detected droplets into 20 size classes (0.75 μm to 10 μm). The particle counts are averaged over 1 s. Throughout the measurement period, the CCN counter operated at a flow rate of 0.5 L min^{-1} with a sheath-to-aerosol flow ratio of 10:1. CCN concentrations were measured at 0.2%, 0.3%, 0.37%, 0.5% and 0.6% supersat-

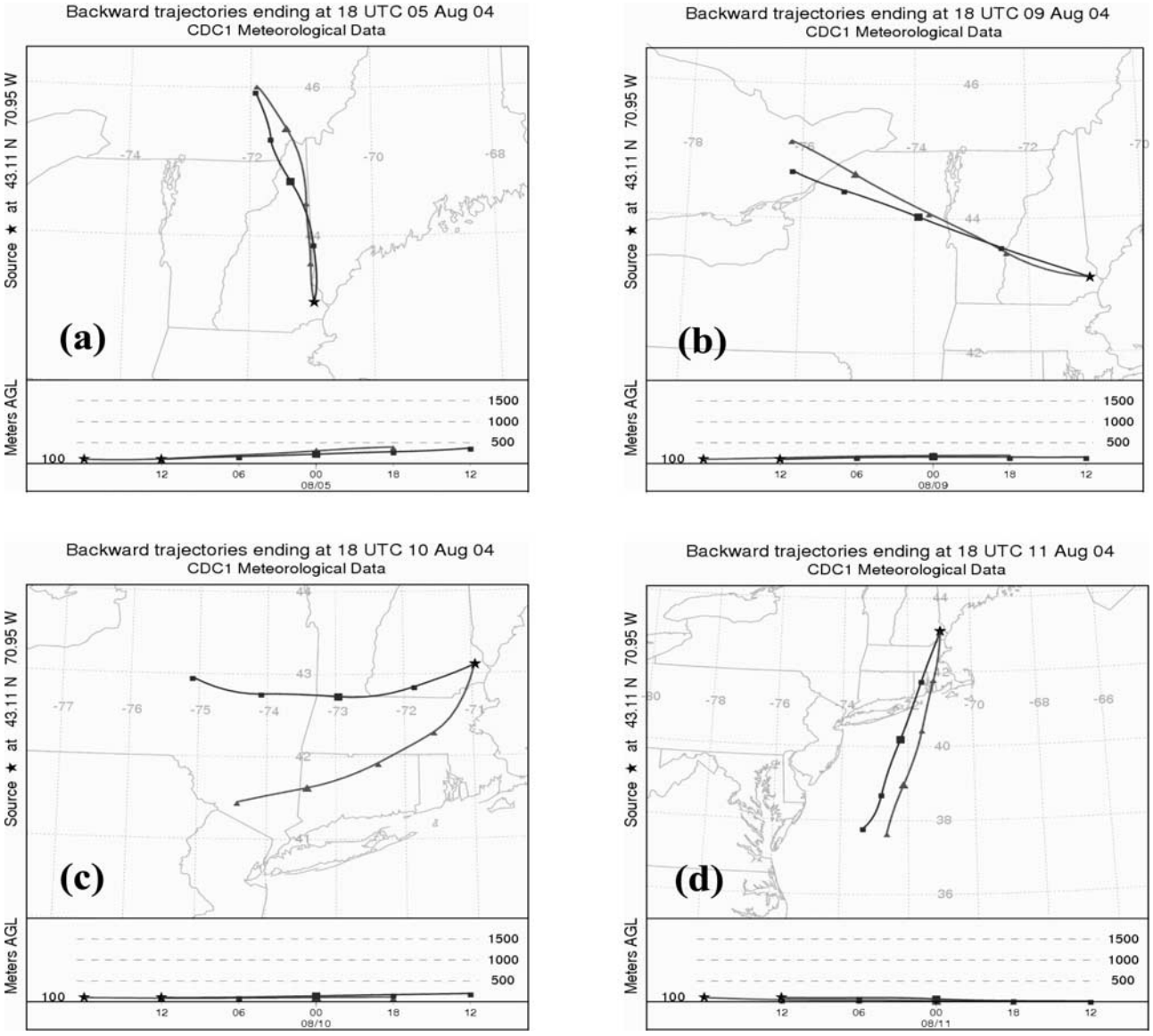

Figure 2. HYSPLIT back trajectories for characteristic types of air masses sampled during the period of interest: (a) 5 August 2004, (b) 9 August 2004, (c) 10 August 2004, and (d) 11 August 2004.

uration. Concentrations were measured at each supersaturation for 6 min, yielding a CCN spectrum every 30 min. We used calibrations with $(NH_4)_2SO_4$ aerosol to characterize the instrument supersaturation; we also operated under conditions for which the droplets had enough time to grow and become distinguishable from the interstitial aerosol.

3. Data Overview

3.1. Air Masses Sampled

[21] Analysis of back trajectories from the HYSPLIT (http://www.arl.noaa.gov/ready/hysplit4.html) model suggests that the air masses sampled at TF from 5 to 8 August resided mostly within the boundary layer throughout its transit from the north (Figure 2a). From 9 to 10 August, boundary layer air from the west was sampled (Figures 2b and 2c), while in the evening of 10 August, the wind direction shifted, transporting southerly boundary layer air (Figure 2d). The daily wind directions are given in Table 1.

3.2. Aerosol Measurements

[22] Figure 3 shows a time series of the total mass loadings (μg m^{-3}) of sulfate and organic measured by the AMS. The inorganic fraction is always dominated by sulfate and ammonium, their relative amounts suggesting that the aerosol is primarily acidic. As a result, nitrate tends to partition in the gas phase, hence the low levels of aerosol nitrate. On 8 August (around 1200 LT), the sulfate mass fraction decreased, leading to partial neutralization of the aerosol and small increase in aerosol nitrate (not shown).

[23] Size-resolved chemical composition was also obtained, for aerosol larger than 80 nm (Figure 4); composition at smaller aerosol sizes was too uncertain, as there was not enough mass to obtain a strong enough signal in the spectrometer. The size-resolved measurements show that

Table 1. Origin of Air Masses Sampled During the Period of Interest

Date	Wind Direction	Air Mass Origin
5 Aug	N	boundary layer
6 Aug	N	boundary layer
7 Aug	N	boundary layer
8 Aug	N	boundary layer
9 Aug	W-WNW	boundary layer
10 Aug	W-WSW	boundary layer
11 Aug	SW-SSW	boundary layer

the sulfate ranges between 20 and 30% for most of the period (Figure 4). The sulfate mass fraction substantially increased between 10 and 11 August (Figure 4), accompanied by a shift of the aerosol size distribution toward larger sizes (Figure 5). The observed shift in chemical composition and size distribution is consistent with the HYSPLIT back trajectories; for most of the period, polluted continental air was sampled, with significant amounts of freshly condensed secondary organic aerosols (SOA) mixing with roughly equal amounts of primary organic carbon (POA) (L. Cottrell et al., manuscript in preparation, 2006). From 10 to 11 August, the air mass was primarily semiurban (i.e., rural aerosol influenced by urban sources), hence the significant increase in sulfate with a size distribution consistent with aged aerosol.

[24] Figure 6 presents the time series of total aerosol (CN) as measured with the SMPS, between 5 and 11 August. For comparison, we present CN measurements from the AIRMAP site CPC (TSI 3010). Overall both instruments follow each other very closely (on average to within 10%).

[25] The total condensation nuclei measurements during the entire campaign averaged about 5000 cm^{-3}. The aerosol concentrations tend to be higher at night and early morning, when the boundary is shallow. Occasionally there are large "spikes" in aerosol concentration, going to as high as 12000 cm^{-3}, likely from the influence of fresh, local combustion emissions (since these events often coincided with large increases in sulfate mass), perhaps with a

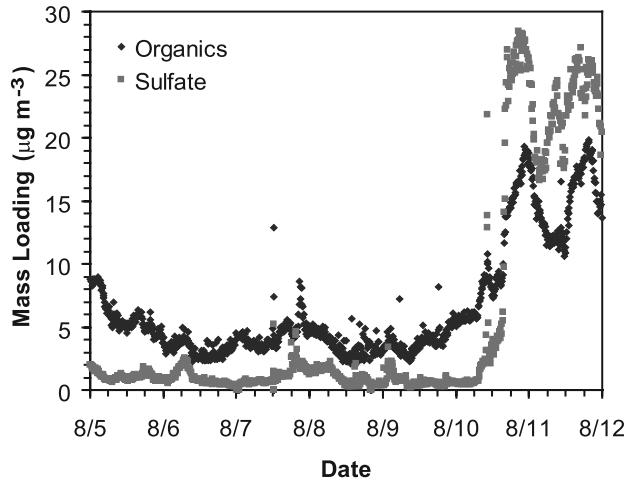

Figure 3. Time series of the total mass loadings from the AMS.

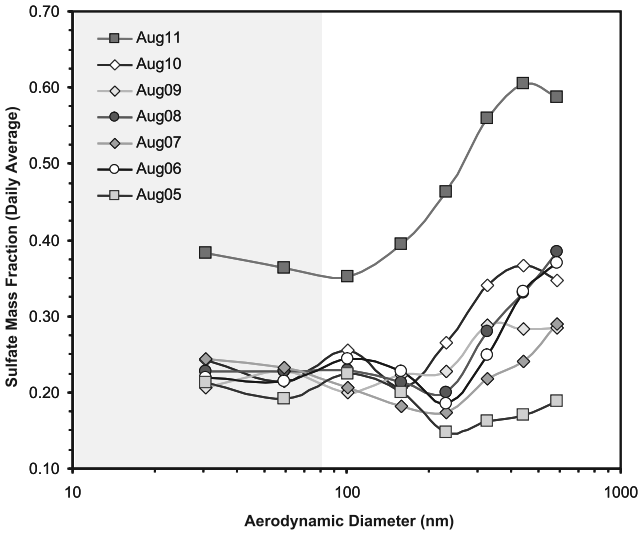

Figure 4. Average sulfate mass fraction size distribution. The shaded region indicates where measurement uncertainty is large.

combination of new particle formation. Throughout most of the measurement period (periods "*A*" and "*B*" in Figure 6), the number distribution peaks somewhere between 70 and 80 nm (Figure 5); this changed in the latter part of the campaign (periods "*C*" in Figure 6), where the aerosol exhibits the characteristic bimodal character of aged aerosol.

3.3. CCN Measurements

[26] The time series of the CCN measurements are superimposed on Figure 6. As expected, the CCN and CN qualitatively track each other, with concentrations being lower as supersaturation decreases. Some of the CN spikes (e.g., around noon on 9 August) are not accompanied by a corresponding peak in the CCN observations, suggesting

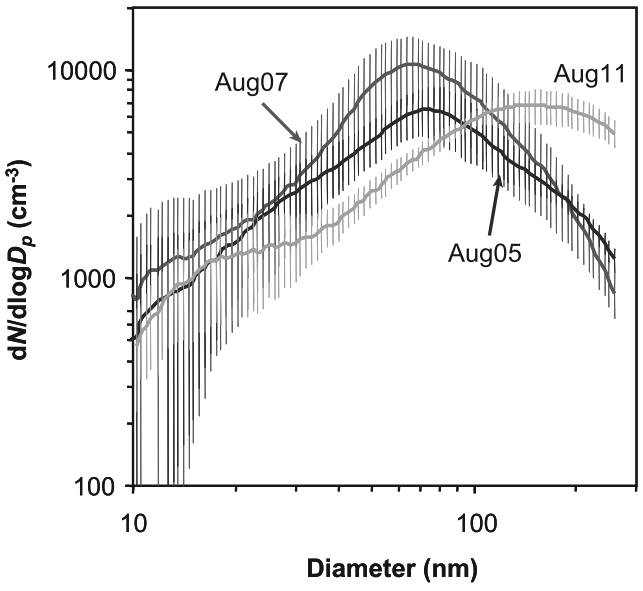

Figure 5. Daily average aerosol size distributions, characteristic of the air masses sampled.

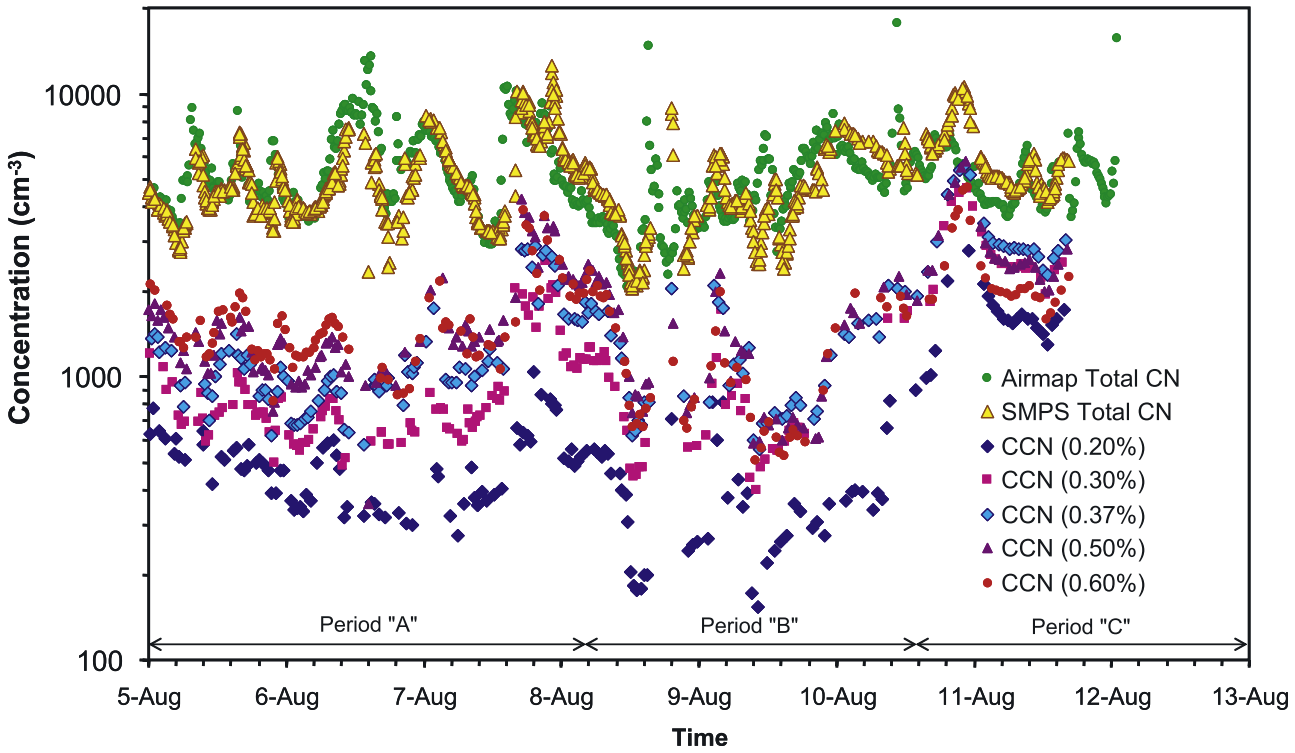

Figure 6. Time series of the CN and CCN measurements throughout the period of interest.

that a fresh combustion source or nucleation event may be responsible for the sudden increase in CN. The subsequent aging of the aerosol and increase in CCN also support this hypothesis.

[27] The CCN concentration time series can be divided into three periods (Figure 6), which coincide with the change in air masses sampled at TF (Figure 2). CCN concentrations increase substantially during period "*C*," while total CN do not; this is consistent with the change in the air masses sampled (Figures 2c and 2d), as semiurban air tends to have more soluble material (i.e., sulfate mass fraction) than continental air, hence are more efficient CCN.

[28] Following the procedure outlined by *Sotiropoulou et al.* [2006], the CCN observations are fit to the "modified power law" CCN spectrum of *Cohard et al.* [1998, 2000],

$$F(s) = \frac{\kappa C s^{\kappa-1}}{(1+\eta s^2)^{\lambda}} \quad (1)$$

where $F(s)$ is the CCN concentration at supersaturation s (i.e., the CCN "spectrum"), C is the total aerosol concentration (cm^{-3}), and κ, η and λ are unitless coefficients determined from the fitting. The numerator in equation (1) is the "power law" expression of *Twomey* [1959]; *Cohard et al.* [1998, 2000] introduced the denominator so that $F(s)$ asymptotes to C at high s ($\approx$10% for ambient aerosol). Table 2 displays the daily and period averages of the CCN spectra. Of all the parameters, C (which scales with total CN) exhibits the largest variability. The other parameters do not vary much at all, suggesting that the normalized CCN spectrum, $\overline{F}(s) = F(s)/C$, is fairly constant throughout the sampling period. Although quite remarkable (given the significant shifts in aerosol size distribution and chemical composition observed between 10 and 11 August), this is largely due to $F(s)$ scaling linearly to C and sublinearly to all the other constants in equation (1). Furthermore, even if the daily averages did not vary much, their uncertainty range became quite large during 5, 6, 9 and 10 August.

4. CCN Closure

[29] Before each closure calculation, the CCN measurements were screened to eliminate biased observations. Each 6-min supersaturation segment is examined for (1) minimal fluctuations in the flow chamber temperature gradient and (2) stability of the flows. Fluctuations in temperature, if small enough, have a minimal impact on instrument supersaturation and closure (B. Ervens et al., Prediction of CCN number concentration using measurements of aerosol size distributions and composition and light scattering enhancement due to humidity, submitted to *Journal of Geophysical Research*, 2006, hereinafter referred to as Ervens et al., submitted manuscript, 2006). If both criteria were satisfied, then the CCN concentrations are averaged over the last 2–3 min of the supersaturation segment (to eliminate the effects of transients when switching supersaturation) and a closure calculation is done. The SMPS size distributions were averaged over each supersaturation segment (we have included only those scans that encompass the times for which CCN measurements were used); instead of fitting the measurements to lognormal distributions (as is often done) we directly use the binned distribution obtained from the SMPS inversion routine. Half-hour averaged aerosol chemical composition is obtained from the AMS data, so there is

Table 2. Daily Averages for CCN Spectra[a]

Date	$C(\times 1000\ \mathrm{cm}^{-3})$	κ	η	λ
5 Aug 2004	4.21 ± 1.01	3.18 ± 0.22	3.13 ± 0.29	1.07 ± 0.08
6 Aug 2004	3.59 ± 0.59	3.34 ± 0.34	3.14 ± 0.14	1.12 ± 0.12
7 Aug 2004	4.14 ± 1.49	3.04 ± 0.09	3.01 ± 0.03	1.02 ± 0.03
8 Aug 2004	2.74 ± 1.00	3.00 ± 0.00	3.00 ± 0.00	1.00 ± 0.00
9 Aug 2004	2.77 ± 0.69	3.09 ± 0.18	3.04 ± 0.07	1.03 ± 0.06
10 Aug 2004	4.75 ± 0.96	3.03 ± 0.07	3.01 ± 0.02	1.01 ± 0.03
11 Aug 2004	3.20 ± 0.32	3.00 ± 0.00	3.00 ± 0.00	1.00 ± 0.00
Period average	3.63 ± 1.17	3.10 ± 0.21	3.05 ± 0.14	1.03 ± 0.07

[a]Parameters correspond to equation (1).

Table 3. Daily CCN Prediction Error Assuming Uniform and Size-Dependent Chemical Composition[a]

Date	% Error Using Uniform ε_s	% Error Using Size-Dependent ε_s
5 Aug 2004	41.37 ± 21.32	16.66 ± 19.18
6 Aug 2004	36.92 ± 27.03	3.07 ± 23.42
7 Aug 2004	26.95 ± 26.81	−0.11 ± 21.28
8 Aug 2004	32.75 ± 25.19	21.23 ± 23.29
9 Aug 2004	43.71 ± 33.68	28.06 ± 30.20
10 Aug 2004	46.76 ± 34.21	30.32 ± 28.13
11 Aug 2004	21.92 ± 28.86	37.93 ± 25.88
Period average	35.71 ± 28.54	17.41 ± 27.05

[a]Unit is %.

one composition measurement for each supersaturation cycle.

[30] When predicting CCN concentrations, we assume that organics do not contribute solute (i.e., are insoluble) nor act as a surfactant. The inorganic fraction of the aerosol is assumed to be ammonium sulfate with an average effective van't Hoff factor, ν_s (which includes an estimate of the osmotic coefficient), of 2.5, obtained from Pitzer activity coefficients [*Brechtel and Kreidenweis*, 2000] for ammonium sulfate CCN with critical supersaturation between 0.2 and 0.6%. The influence of other inorganic species (e.g., nitrate) is negligible. The critical supersaturation, s_c for each particle with dry size d, is calculated from Köhler theory [*Seinfeld and Pandis*, 1998],

$$s_c = \left[\frac{256}{27}\left(\frac{M_w\sigma}{RT\rho_w}\right)^3\left(\frac{M_s}{\rho_s}\right)\left(\frac{\rho_w}{M_w}\right)\frac{d^3}{\varepsilon_s\nu_s}\right]^{1/2} \quad (2)$$

where R is the universal gas constant, T is the ambient temperature, σ is the surface tension of the CCN at the point of activation (assumed here to be equal to that of water), M_s is the molar mass of the solute and M_w, ρ_w are the molar mass and density of water, respectively. The volume fraction of solute, ε_s, can be calculated as a function of the mass fraction of solute, m_s and its density, ρ_s,

$$\varepsilon_s = \frac{\frac{m_s}{\rho_s}}{\frac{m_s}{\rho_s} + \frac{1-m_s}{\rho_i}} \quad (3)$$

where ρ_i is the density of the insoluble organic (here assumed 1500 kg m^{-3}). Particles are counted as CCN when their s_c is less or equal than the supersaturation of the CCN counter. The predicted and measured CCN are then compared to assess closure.

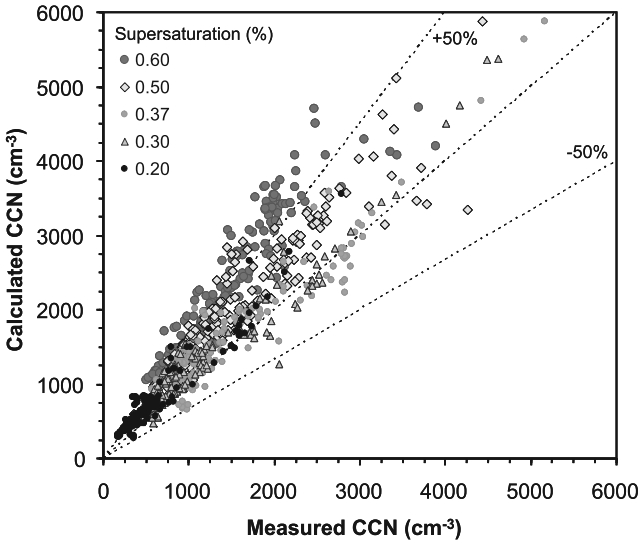

Figure 7. Calculated versus measured CCN concentrations. Size-averaged ε_s is used for the calculations.

4.1. Size-Averaged Chemical Composition

[31] The CCN closure using size-averaged chemical composition (which is computed by weighing the composition of each CCN by their concentration) is shown in Figure 7. The individual closure calculations are color-coded by supersaturation. Figure 7 clearly shows that there is a tendency for overprediction; for 0.2%, 0.3%, 0.37%, 0.5% and 0.6% supersaturation, the prediction error is 37.2 ± 28.2%, 22.0 ± 21.4%, 16.9 ± 23.1%, 37.7 ± 20.8% and 64.2 ± 22.6%, respectively (average error 35.8 ± 28.5%). The CCN closure worsens (average error >40%) during 5, 9, and 10 August (Table 3), which correspond to days with shifting wind direction (Table 1). If the organic fraction is assumed to be soluble, the CCN prediction error would be even larger. Not accounting for size-resolved composition and aerosol mixing state are prime sources of CCN prediction error. The former is addressed below.

4.2. Size-Dependent Chemical Composition

[32] The size-dependent CCN closure is shown in Figure 8. The individual closure calculations are color-coded by supersaturation. Compared to the size-averaged closure (Figure 7), specifying size-dependent chemical composition substantially improves predictions; for 0.2%, 0.3%, 0.37%, 0.5% and 0.6% supersaturation, the prediction error is 21.3 ± 30.0%, 5.2 ± 17.0%, 1.5 ± 18.4%, 15.6 ± 19.8% and 43.3 ± 26.0%, respectively (average error 17.4 ± 27.0%). The closure at 0.6% is considerably worse than for the other supersaturations; this is likely from lack of chemical composition measurements below 80 nm size (many of the CCN at 0.6% are from smaller sizes).

[33] Compared to the size-averaged closure, specifying size-dependent chemical composition substantially improves the closure for all days except 11 August (Table 3). CCN closure is worst (average error >25%) during 9, 10 and 11 August (Table 1). The average error on 11 August is

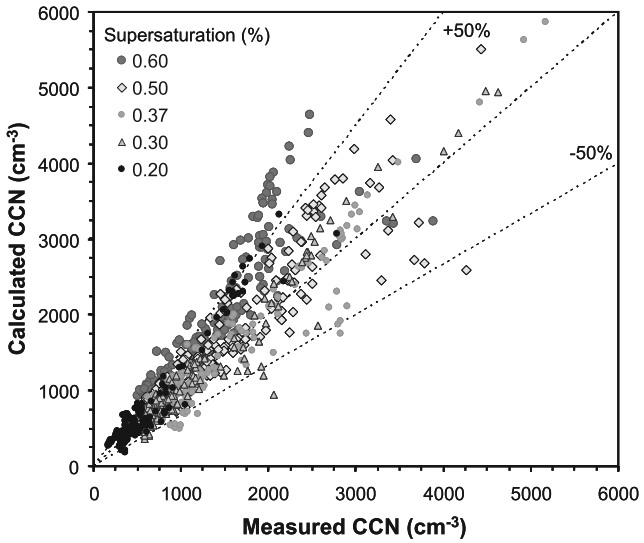

Figure 8. Calculated versus measured CCN concentrations. Size-dependent ε_s is used for the calculations.

somewhat high, largely from the discrepancy in CCN predictions at 0.6%. Like in the size-averaged closure, 9 and 10 August correspond to days with shifting wind direction (Table 1). If the organic fraction is assumed to be soluble, the CCN prediction error would increase. Since size-dependent chemical composition is considered in the closure, the assumption of internally mixed aerosol is likely a key source of the residual error. This is addressed in a companion manuscript (A. Nenes and J. Medina, manuscript in preparation, 2006).

5. Summary and Conclusions

[34] Concurrent measurements of CCN (at 0.2%, 0.3%, 0.37%, 0.5% and 0.6% supersaturation), aerosol size distribution and chemical composition were carried out at the UNH-AIRMAP Thompson Farms site, during the ICARTT 2004 campaign. This work focuses on a week of measurements (5–11 August 2004) for assessment of CCN closure. The aerosol sampled in this study was either polluted continental from the Great Lakes area, or semiurban from south of the sampling site. The aerosol measured exhibits the characteristics expected for each type of aerosol; the polluted continental air tends to have high concentrations of small particles, and contain large amounts of organics. Semiurban tends to have larger CCN, and higher sulfate mass fraction. The aerosol was assumed to be composed of an insoluble and soluble fraction.

[35] CCN concentrations are calculated using the measured aerosol size distribution and chemical composition coupled with "simple" Köhler theory. Predictions are then compared with measurements for supersaturations ranging between 0.2% and 0.6% and a variety of air masses sampled. Using size-averaged chemical composition, CCN are overpredicted on average by 35.8 ± 28.5%. Introducing size-dependent chemical composition substantially improved closure (average error 17.4 ± 27.0%), although CCN concentrations still tend to be overpredicted. CCN closure is worse during periods of changing wind direction; this suggests that aerosol mixing state may need to be considered to improve CCN predictions. Introducing organic solubility and surface tension depression would worsen CCN closure. To the extent where our analysis applies, this suggests that organics may not contribute substantial amounts of solute.

[36] Overall our study suggests that "simple" Köhler theory can be used to predict CCN concentrations; most of the discrepancies are addressed if size-dependent soluble salt fraction is known. Although organics can potentially have a strong influence on cloud droplet formation (e.g., in biomass burning aerosol), it seems that knowledge of the soluble salt fraction is sufficient for description of CCN activity at Thompson Farms. The latter finding is consistent with similar closure studies conducted in the past [e.g., *Liu et al.*, 1996; *Broekhuizen et al.*, 2006] and those released during the ICARTT [*Fountoukis et al.*, 2006; Ervens et al., submitted manuscript, 2006].

[37] Our measurements can be used to constrain the uncertainty associated with common assumptions in GCM modeling studies of the aerosol indirect effect. For example, *Sotiropoulou et al.* [2006], using the observations presented herein, estimate a 25% error in global cloud droplet number arising from the application of "simple" Köhler theory. This suggests that the estimated uncertainty in indirect forcing is -0.5 W m^{-2}, or about a third of the total indirect forcing [*IPCC*, 2001]. A full assessment requires the application of a global model and will be the focus of a future study.

[38] **Acknowledgments.** This work was supported by NOAA under grant NA04OAR4310088, an NSF CAREER award and a Blanched-Million Young Faculty Fellowship. J. M. acknowledges support from a NASA Earth System Science Fellowship. UNH acknowledges funding of NOAA AIRMAP grants NA03OAR4600122 and NA04OAR4600154. We also acknowledge the support from G. Kok (DMT), and the G. Huey research group (Georgia Tech).

References

Abdul-Razzak, H., and S. Ghan (2000), A parameterization of aerosol activation: 2. Multiple aerosol types, *J. Geophys. Res.*, *105*, 6837–6844.

Abdul-Razzak, H., and S. J. Ghan (2002), A parameterization of aerosol activation: 3. Sectional representation, *J. Geophys. Res.*, *107*(D3), 4026, doi:10.1029/2001JD000483.

Alfarra, R., H. Coe, J. Allan, K. Bower, H. Boudries, M. Canagaratna, J. Jimenez, J. Jayne, A. Garforth, S. Li, and D. Worsnop (2004), Characterization of urban and regional organic aerosols in the Lower Fraser Valley using two Aerodyne aerosol mass spectrometers, *Atmos. Environ.*, *38*, 5745–5758.

Allan, J. D., J. L. Jimenez, P. I. Williams, M. R. Alfarra, K. N. Bower, J. T. Jayne, H. Coe, and D. R. Worsnop (2003), Quantitative sampling using an Aerodyne aerosol mass spectrometer: 1. Techniques of data interpretation and error analysis, *J. Geophys. Res.*, *108*(D3), 4090, doi:10.1029/2002JD002358.

Brechtel, F. J., and S. M. Kreidenweis (2000), Predicting particle critical supersaturation from hygroscopic growth measurements in the humidified TDMA. Part I: Theory and sensitivity studies, *J. Aerosol Sci.*, *57*, 1854–1871.

Broekhuizen, K., R. Chang, W. Leaitch, S. Li, and J. P. D. Abbatt (2006), Closure between measured and modeled cloud condensation nuclei (CCN) using size-resolved aerosol compositions in downtown Toronto, *Atmos. Chem. Phys.*, *6*, 2513–2524.

Cantrell, W., G. Shaw, G. Cass, Z. Chowdhury, L. Hughes, K. Prather, S. Guazzotti, and K. Coffee (2001), Closure between aerosol particles and cloud condensation nuclei at Kaashidhoo climate observatory, *J. Geophys. Res.*, *106*(D22), 28,711–28,718.

Charlson, R., S. Schwartz, J. Hales, R. Cess, J. Coakley, J. Hansen, and D. Hofmann (1992), Climate forcing by anthropogenic aerosols, *Science*, *255*, 6423–6430.

Chuang, P., D. Collins, H. Pawlowska, J. Snider, H. Jonsson, J. L. Brenguier, R. Flagan, and J. Seinfeld (2000a), CCN measurements during ACE-2 and their relationship to cloud microphysical properties, *Tellus, Ser. B*, *52*, 843–867.

Chuang, P., A. Nenes, J. Smith, R. Flagan, and J. Seinfeld (2000b), Design of a CCN instrument for airborne measurement, *J. Atmos. Oceanic Technol.*, *17*, 1005–1019.

Cohard, J., J. Pinty, and C. Bedos (1998), Extending Twomey's analytical estimate of nucleated cloud droplet concentrations from CCN spectra, *J. Atmos. Sci.*, *55*, 3348–3357.

Cohard, J., J. Pinty, and K. Suhre (2000), On the parameterization of activation spectra from cloud condensation nuclei microphysical properties, *J. Geophys. Res.*, *105*, 11,753–11,766.

Collins, D., A. Nenes, R. Flagan, and J. Seinfeld (2000), The scanning flow DMA, *J. Aerosol Sci.*, *31*, 1129–1144.

Covert, D., J. Gras, A. Wiedensohler, and F. Stratmann (1998), Comparison of directly measured CCN with CCN modeled from the number-size distribution in the marine boundary layer during ACE 1 at Cape Grim, Tasmania, *J. Geophys. Res.*, *103*(D13), 16,597–16,608.

Decesari, S., M. C. Facchini, M. Mircea, F. Cavalli, and S. Fuzzi (2003), Solubility properties of surfactants in atmospheric aerosol and cloud/fog water samples, *J. Geophys. Res.*, *108*(D21), 4685, doi:10.1029/2003JD003566.

Delene, D., and T. Deshler (2000), Calibration of a photometric cloud condensation nucleus counter designed for deployment on a balloon package, *J. Atmos. Oceanic Technol.*, *17*, 459–467.

Dusek, U., D. Covert, A. Wiedensohler, C. Neususs, D. Weise, and W. Cantrell (2003), Cloud condensation nuclei spectra derived from size distributions and hygroscopic properties of the aerosol in coastal southwest Portugal during ACE-2, *Tellus, Ser. B*, *55*, 35–53.

Facchini, M., M. Mircea, S. Fuzzi, and R. Charlson (1999), Cloud albedo enhancement by surface-active organic solutes in growing droplets, *Nature*, *401*, 257–259.

Fountoukis, C., and A. Nenes (2005), Continued development of a cloud droplet formation parameterization for global climate models, *J. Geophys. Res.*, *110*, D11212, doi:10.1029/2004JD005591.

Fountoukis, C., et al. (2006), Aerosol–cloud drop concentration closure for clouds sampled during ICARTT, *J. Geophys. Res.*, doi:10.1029/2006JD007272, in press.

Haywood, J., and O. Boucher (2000), Estimates of the direct and indirect radiative forcing due to tropospheric aerosols: A review, *Rev. Geophys.*, *38*(4), 513–543.

Intergovernmental Panel on Climate Change (2001), *Climate Change 2001: The Scientific Basis*, Cambridge Univ. Press, New York.

Jayne, J., D. Leard, X. Zhang, P. Davidovits, K. Smith, C. Kolb, and D. Worsnop (2000), Development of an aerosol mass spectrometer for size and composition analysis of submicron particles, *Aerosol Sci. Technol.*, *33*, 49–70.

Ji, Q., G. Shaw, and W. Cantrell (1998), A new instrument for measuring cloud condensation nuclei: Cloud condensation nucleus "remover," *J. Geophys. Res.*, *103*, 28,013–28,019.

Jimenez, J. L., et al. (2003), Ambient aerosol sampling using the Aerodyne Aerosol Mass Spectrometer, *J. Geophys. Res.*, *108*(D7), 8425, doi:10.1029/2001JD001213.

Köhler, H. (1921), Zur kondensation des wasserdampfe in der atmosphäre, *Geofys. Publ.*, *2*, 3–15.

Köhler, H. (1936), The nucleus in the growth of hygroscopic droplets, *Trans. Faraday Soc.*, *32*, 1152.

Lance, S., J. Medina, J. Smith, and A. Nenes (2006), Mapping the operation of the DMT continuous flow CCN counter, *Aerosol Sci. Technol.*, *40*, 242–254.

Liu, P., W. Leaitch, C. Banic, S. Li, D. Ngo, and W. Megaw (1996), Aerosol observations at Chebogue Point during the 1993 North Atlantic Regional Experiment: Relationships among cloud condensation nuclei, size distribution, and chemistry, *J. Geophys. Res.*, *101*, 28,971–28,990.

Nenes, A., and J. H. Seinfeld (2003), Parameterization of cloud droplet formation in global climate models, *J. Geophys. Res.*, *108*(D14), 4415, doi:10.1029/2002JD002911.

Nenes, A., P. Chuang, R. Flagan, and J. Seinfeld (2001), A theoretical analysis of cloud condensation nucleus (CCN) instruments, *J. Geophys. Res.*, *106*, 3449–3474.

Nenes, A., R. J. Charlson, M. C. Facchini, M. Kulmala, A. Laaksonen, and J. H. Seinfeld (2002), Can chemical effects on cloud droplet number rival the first indirect effect?, *Geophys. Res. Lett.*, *29*(17), 1848, doi:10.1029/2002GL015295.

Ramanathan, V., P. Crutzen, J. Kiehl, and D. Rosenfeld (2001), Aerosols, climate, and the hydrological cycle, *Science*, *294*, 2119–2124.

Rissman, T. A., T. M. VanReken, J. Wang, R. Gasparini, D. R. Collins, H. H. Jonsson, F. J. Brechtel, R. C. Flagan, and J. H. Seinfeld (2006), Characterization of ambient aerosol from measurements of cloud condensation nuclei during the 2003 Atmospheric Radiation Measurement Aerosol Intensive Observational Period at the Southern Great Plains site in Oklahoma, *J. Geophys. Res.*, *111*, D05S11, doi:10.1029/2004JD005695.

Roberts, G., and A. Nenes (2005), A continuous-flow streamwise thermal-gradient CCN chamber for atmospheric measurements, *Aerosol Sci. Technol.*, *39*, 206–221.

Roberts, G. C., A. Nenes, J. H. Seinfeld, and M. O. Andreae (2003), Impact of biomass burning on cloud properties in the Amazon Basin, *J. Geophys. Res.*, *108*(D2), 4062, doi:10.1029/2001JD000985.

Seinfeld, J., and S. Pandis (1998), *Atmospheric Chemistry and Physics: From Air Pollution to Climate Change*, John Wiley, Hoboken, N. J.

Shulman, M., M. Jacobson, R. Charlson, R. Synovec, and T. Young (1996), Dissolution behaviour and surface tension effects of organic compounds in nucleating cloud droplets, *Geophys. Res. Lett.*, *23*, 277–280.

Snider, J., S. Guibert, J. Brenguier, and J. Putaud (2003), Aerosol activation in marine stratocumulus clouds: 2. Köhler and parcel theory closures studies, *J. Geophys. Res.*, *108*(D15), 8629, doi:10.1029/2002JD002692.

Sotiropoulou, R.-E. P., J. Medina, and A. Nenes (2006), CCN predictions: Is theory sufficient for assessments of the indirect effect?, *Geophys. Res. Lett.*, *33*, L05816, doi:10.1029/2005GL025148.

Stroud, C., et al. (2006), Cloud activating properties of aerosol observed during CELTIC, *J. Atmos. Sci.*, *64*(2), 441–459.

Twomey, S. (1959), The nuclei of natural cloud formation. II. The supersaturation in natural clouds and the variation of cloud droplet concentration, *Geofis. Pura Appl.*, *43*, 243–249.

VanReken, T. M., T. A. Rissman, G. C. Roberts, V. Varutbangkul, H. H. Jonsson, R. C. Flagan, and J. H. Seinfeld (2003), Toward aerosol/cloud condensation nuclei (CCN) closure during CRYSTAL-FACE, *J. Geophys. Res.*, *108*(D20), 4633, doi:10.1029/2003JD003582.

Zhang, Q., M. R. Canagaratna, J. T. Jayne, D. R. Worsnop, and J.-L. Jimenez (2005), Time- and size-resolved chemical composition of submicron particles in Pittsburgh: Implications for aerosol sources and processes, *J. Geophys. Res.*, *110*, D07S09, doi:10.1029/2004JD004649.

P. J. Beckman, L. D. Cottrell, R. J. Griffin, and L. D. Ziemba, Institute for the Study of Earth, Oceans, and Space, University of New Hampshire, Durham, NH 03824, USA. (pbeckman@gust.sr.unh.edu; lauradcottrell@yahoo.com; rjg@gust.sr.unh.edu; lziemba@cisunix.unh.edu)

J. Medina, School of Chemical and Biomolecular Engineering, Georgia Institute of Technology, Atlanta, GA 30332, USA. (jeessy.medina@chbe.gatech.edu)

A. Nenes (corresponding author) and R. E. P. Sotiropoulou, School of Earth and Atmospheric Sciences, Georgia Institute of Technology, Atlanta, GA 30332, USA. (nenes@eas.gatech.edu; rsot@eas.gatech.edu)